

1 Virulence and pangenome analysis of *Vibrio harveyi* strains from Greek
2 and Red Sea marine aquaculture

3

4 Adriana Triga^{1,2}, Zeenat Atinuke Issa^{1,2}, Maria Smyrli¹, Linda Fenske³, Pantelis Katharios¹

5

6 1. Institute of Marine Biology, Biotechnology and Aquaculture (IMBBC), Hellenic Centre for Marine
7 Research (HCMR), P.O. Box 2214, 71500 Heraklion, Greece

8 2. Department of Biology, University of Crete, P.O. Box 1470, 71110 Heraklion, Greece

9 3. Bioinformatics & Systems Biology, Justus Liebig University Gießen, 35390 Gießen, Hesse,
10 Germany

11

12 Correspondence:

13 katharios@hcmr.gr

14 Institute of Marine Biology, Biotechnology and Aquaculture (IMBBC)

15 Hellenic Centre for Marine Research (HCMR)

16 Thalassocosmos, Ex-US base

17 P.O.Box 2214

18 715 00 Gournes, Heraklion, Crete

19 Greece

20

21 **Abstract**

22

23 Comparative genomic analysis of *Vibrio harveyi*, a leading pathogen in Mediterranean aquaculture, was
24 conducted to assess the genomic plasticity of the species. *V. harveyi* is responsible for vibriosis outbreaks
25 during the warmer months, resulting in significant economic losses that impact Greek aquaculture. Over a
26 span of six years, we curated a diverse collection of bacterial strains associated with these outbreaks. Whole-
27 genome sequencing was employed in 21 strains to uncover their evolutionary relationships and virulence
28 factors. Pangenome analysis revealed significant gene gain/loss, with numerous unique genes within the
29 strains. The core genome featured genes associated with pathogenicity, including secretion systems,
30 flagella, pili, siderophores, and toxins. Furthermore, we examined the phenotypic traits and virulence of
31 these strains using *in vivo* testing with gilthead seabream larvae. Our findings indicated variant metabolic
32 profiles and virulence among the strains during these *in vivo* assays. By integrating genomic and phenotypic
33 data, our study highlights the ongoing evolution of disease-associated *V. harveyi* strains, which pose a
34 growing challenge to the aquaculture industry.

35

36 **Keywords**

37 *Vibrio harveyi*, comparative genomics, pangenome, virulence, marine aquaculture

38

39 **1. Introduction**

40

41 *Vibrio* spp. encompass a group of bacteria that are highly prevalent in aquatic environments,
42 displaying adaptability to a broad spectrum of salinities and temperatures. This versatility has
43 enabled them to inhabit a diverse array of ecological niches, including anthropogenic environments

44 like wastewater and aquaculture systems (Baker-Austin et al., 2017; Le Roux et al., 2015). They
45 thrive in anaerobic/aerobic, oligotrophic/nutrient-rich conditions, in biofilms and sediments, as
46 free-living cells, or associated with different hosts. This adaptability has been attributed to their
47 wide variety of genes and metabolic pathways. *Vibrios* can have various hosts, from microalgae
48 to vertebrates, and they act as symbionts or pathogens (Mougin et al., 2021; Sampaio et al., 2022).
49 Vibriosis is one of the oldest known diseases of fish, causing enormous economic losses to the
50 marine aquaculture industry (Mohd Yazid et al., 2021; Roberts, 2012). *V. harveyi* is one of the
51 species related to the disease and it can infect a wide range of fishes, including the catfish, grouper,
52 the rainbow trout, breams and basses (Austin and Zhang, 2006). The most relevant clinical signs
53 of vibriosis in fish include the presence of hemorrhages, skin lesions, fin erosion, ulceration and
54 gastro-enteritis. It can also cause systemic infection and mortality in fish, leading to septicemia
55 and organ failure (Mohamad et al., 2019; Zhang et al., 2020). The species is also notable for
56 causing mass mortalities in crustacean and mollusks aquaculture with systemic and severe
57 symptoms in shrimps, lobsters, oysters and abalones (Meibom et al., 2005; Saulnier et al., 2010;
58 Sawabe et al., 2007).

59 The *Vibrio* genus exhibits great genome plasticity within its members, even within populations of
60 the same species (Le Roux and Blokesch, 2018). In addition, among the different pathogens able
61 to colonize many niches, has disproportionately more virulence factors inside genomic islands
62 (GIs) (Ho Sui et al., 2009) underpinning how horizontal gene transfer (HGT) has created a
63 reservoir of genetic tools, readily available for use when an evolutionary cue arises. In the present
64 study, 21 new genomes mainly deriving from the European seabass are presented. Other fin fishes
65 that served as hosts were aquaculture species from the Mediterranean, such as the gilthead
66 seabream (*Sparus aurata*), the greater amberjack (*Seriola dumerili*), and the common dentex

67 (*Dentex dentex*). Moreover, two strains isolated from marine farms from the Red Sea were included
68 in the study, one from gilthead seabream and one from Nile tilapia (*Oreochromis niloticus*). We
69 conducted a comprehensive genome-wide comparison to elucidate both similarities and strain-
70 specific characteristics. The analysis focused on virulence and antibiotic resistance, and genomic
71 data were correlated with phenotypic traits. We present this set of draft genomes as a pangenome
72 of *V. harveyi* strains causing disease in marine fishes.

73

74 **2. Materials and Methods**

75

76 **2.1 Sampling and Strain Isolation, Microbiology and Virulence**

77

78 The *V.harveyi* strains described in this study are all isolates from clinical cases and derived from
79 5 fish species, the *Dicentrarchus labrax*, *Sparus aurata*, *Seriola dumerili*, *Dentex dentex*, and
80 *Oreochromis niloticus*. They are members of a wider collection resulted from a big sampling effort
81 to study vibriosis caused by *V. harveyi* in Greece which has been published previously by our team
82 (Triga et al., 2023). The bacterial strains used here were routinely isolated on TCBS agar and then
83 re-cultures were purified on Tryptone Soy Agar (TSA) supplemented with 2% NaCl. All strains
84 were further cultured on Difco Marine Agar (MA) (Becton, Dickinson and Company, Le Pont de
85 Claix, France), MacConkey-AMP-Tween agar (Sigma-Aldrich, Co., St. Louis, MO, USA), MIO
86 media (Sigma-Aldrich, Co., St. Louis, MO, USA) and 5% seabass blood agar (blood taken from
87 healthy fish of the broodstock in the HCMR facilities). The phenotypic fingerprint of the strains
88 was obtained using the GEN III MicroPlate (BIOLOG, Hayward, USA) kit. Antibiotic

89 susceptibility to antibiotics relevant to aquaculture practice was assessed with the disc diffusion
90 method according to CLSI M45 guidelines on Mueller-Hinton agar (MHA) (Difco, USA)
91 supplemented with 2% NaCl (CLSI, 2016). The antibiotic susceptibility discs (Oxoid Ltd.
92 Basingstoke, Hampshire, England) were ampicillin 10 µg (AMP10), oxolinic acid 2 µg (OA2),
93 flumequine 30 µg (UB30), florfenicol 30 µg (FFC30), oxytetracycline 30 µg (OT30) and
94 sulfamethoxazole/ trimethoprim 25 µg (SXT25). The gilthead seabream (*Sparus aurata*) larvae
95 model was used to compare the virulence of the 21 strains *in vivo* as described in Droubogiannis
96 *et al.* (Droubogiannis and Katharios, 2022) using eggs acquired from the HCMR broodstock
97 facility. Briefly, gilthead seabream eggs were placed individually in 96-well plates in sterile
98 seawater after being washed three times in sterile seawater. Infection was initiated after hatching
99 of all larvae, with the addition of 20 µL of bacterial suspensions of the strain tested adjusted to
100 achieve a mean final concentration of 1.66×10^6 cfu ml⁻¹ in the wells. Mortality of the fish larvae
101 was monitored over a period of 5 days. The 96-well plates were incubated at a constant temperature
102 of 22°C in a cooling incubator. Kaplan-Meier survival curves and statistical analysis were
103 calculated using GraphPad Prism 10.0.0 (GraphPad Software, Boston, Massachusetts USA,
104 www.graphpad.com).

105

106 2.2 Genomic DNA Extraction, Whole Genome Sequencing, Genome Assembly and 107 Annotation

108

109 Overnight cultures (25°C in TSB 2% NaCl) of the strains were processed with the DNeasy Blood
110 and Tissue kit (QIAGEN, Hilden, Germany) for DNA extraction, followed by quality control using

111 NanoDrop (Thermo Fisher Scientific, Waltham, MA, USA), Qubit (Thermo Fisher Scientific,
112 Waltham, MA, USA) instruments and 1% agarose gel electrophoresis. Whole genome sequencing
113 was conducted in the DNBseq platform (BGI Tech Solutions, Hong Kong) on the DNBSEQ-G400
114 sequencer using paired-end technology (PE100). The library preparation and filtering procedure
115 was done according to previously described method (Tsertou et al., 2023). The PATRIC platform
116 (Davis et al., 2019) was utilized for the genome assembly, and the following tools were involved
117 in the pipeline: Samtools 1.3 (Danecek et al., 2021), the Unicycler v0.4.8 (Wick et al., 2017), Pilon
118 1.23 (Walker et al., 2014) and Bandage 0.8.1 (Wick et al., 2015). The assembly was assessed with
119 BUSCO (Simão et al., 2015) and then the contigs were submitted to the GenBank and annotated
120 by the NCBI Prokaryotic Genome Annotation Pipeline (PGAP) (Li et al., 2021). Plasmid
121 sequences were explored with PLACNETw (Vielva et al., 2017). The corrected reads were also
122 submitted to the Sequence Read Archive (SRA) database, accession numbers are presented in
123 **Table 1**. The VH2 draft genome has been already published (Castillo et al., 2015), but for sake of
124 comparison and the same workflow being followed for all genomes, it got re-sequenced.

125

126 2.3 Pangenome analysis and Phylogeny

127

128 The pangenome analysis was performed in the web-based platform for comparative genomics
129 “Efficient Database framework for comparative genome analyses using BLAST score Ratios”
130 EDGAR 3.0 (<https://edgar3.computational.bio.uni-giessen.de>) (Dieckmann et al., 2021). In
131 EDGAR, the development of the pangenome was computed, along with the distribution and
132 categorization of gene sets into core, dispensable, and singletons. The core subset refers to the set
133 of genes present in all strains of a given species or population, representing the conserved genomic

134 content. The dispensable subset comprises genes present in some, but not all, strains, indicating
135 variability within the population. Singleton genes are unique to individual strains, representing
136 strain-specific elements. The construction of an approximately-maximum-likelihood phylogenetic
137 tree was done after alignment of all core gene sets using MUSCLE (Edgar, 2004), and then with
138 the FastTree software (<http://www.microbesonline.org/fasttree/>), as it is more discriminatory and
139 effective than multi-locus or 16S rRNA based analysis. The genome similarity ANI-matrix was
140 calculated with the Genome-based Distance Matrix calculator (Rodriguez-R and Konstantinidis,
141 2016), also including the *V. harveyi* reference strain ATCC 33843 (392 MAV), NCBI Biosample
142 SAMN03075601. The EDGAR platform offered the construction of circular plot of the genes of
143 the genomes using BioCircos (Cui et al., 2016) and the calculation of a POCP (percentage of
144 conserved proteins) (Qin et al., 2014) matrix to estimate their evolutionary and phenotypic
145 distance. In the EDGAR analyses that required a reference genome for the iterative calculation and
146 the gene order of the output, VhP1-sp was set as one, as it was one of the oldest isolated strains.
147 The multi-locus sequence typing (MLST) was used to allocate a sequence type for the 21 strains,
148 and the isolates' alleles were submitted to the Public Databases for Molecular Typing and
149 Microbial Genome Diversity (Jolley et al., 2018).

150

151 2.4 Functional annotations

152

153 The PATRIC workspace was employed for detecting virulence factors, and antibiotic resistance
154 genes (ARGs), the CRISPRCasFinder v1.1.2 (Couvin et al., 2018) for CRISPR-Cas systems in the
155 strains and DefenseFinder (Tesson et al., 2022) for anti-phage systems search. Gene sets of the
156 pangenome were further analyzed with VFDB (Chen, 2004), EDGAR 3.0 and BlastKOALA

157 (Kanehisa et al., 2016) for functional category analysis. Genomic islands (GIs) were predicted with
158 the webtool IslandViewer v4 (Bertelli et al., 2017) using two independent methods that supported
159 the assembly level of the genomes, the SIGI-HMM and IslandPath-DIMOB, after the ordering of
160 the contigs against the reference genome *V. harveyi* ATCC 33843 (392 MAV). From the results
161 produced, the GIs not aligned to the reference were filtered out. Prophage regions were identified
162 and annotated using the PHASTER webserver (Arndt et al., 2016). The prophage regions located
163 at the end of the contigs were assigned manually as incomplete.

164

165 **3. Results and Discussion**

166

167 **3.1 Strain Biochemical Characterization**

168

169 The 21 *V. harveyi* strains produced yellow colonies on the TCBS, and colorless to yellowish on
170 the MacConkey-AMP-Tween. They were all defined as motile in the MIO medium, had negative
171 phenotype for indole production, and 61% were positive for the ornithine decarboxylase (ODC)
172 (**Table S1**). A negative phenotype for ODC has been reported for other *V. harveyi* isolates (Brenner
173 et al., 2005; Pavlinec et al., 2022). Indole is an important intercellular signal molecule, produced
174 by many bacteria including vibrios and *V. harveyi* (Lee and Lee, 2010). When present in the
175 extracellular space, indole plays a role in decreasing the formation of biofilm and the virulence of
176 pathogenic *Vibrio* spp. (Li et al., 2014; Mueller et al., 2009; Zhang et al., 2022).

177 The Gen III MicroPlate assay results unveiled various carbon-utilization phenotypes. All strains
178 were cultivated within the tested NaCl gradient (2-8% NaCl) (Brenner et al., 2005). They exhibited

179 metabolic activity towards several substrates, including D-glucuronic acid, a constituent of
180 capsular polysaccharides (Riegert et al., 2021) and other bacterial and algae structures (Vinnitskiy
181 et al., 2015), as well as N-acetyl-D-glucosamine, a component of peptidoglycan and chitin.
182 Additionally, these strains metabolized the amino acids L-glutamic acid, L-serine, L-alanine, and
183 D-mannitol, commonly present in seaweed. These phenotypic profiles provide insights into the
184 degree of adaptation of *V. harveyi* isolates to the marine environment. Notably, there was
185 significant diversity in other metabolic traits, with 90% of isolates capable of fermenting sucrose,
186 14% metabolizing D-salicin, 86% utilizing D-cellobiose, and 67% D-galactose. Additionally, 33%
187 of the strains utilized L-arginine. However, none of the isolates exhibited the ability to utilize myo-
188 inositol, D-melibiose, or formic acid. It is noteworthy that formic acid has inhibitory properties
189 against various vibrios, including *V. harveyi*, and has been utilized as a bio-control agent against
190 vibriosis, particularly in shrimp aquaculture (Adams and Boopathy, 2013; Chuchird et al., 2015).

191 In the chemical resistance assays of Gen III MicroPlate, all of them showed growth at pH=6, and
192 four at pH=5, the Gal 90, ML 1, SA 6.1 and Sernef. The strains were sensitive to minocycline and
193 nalidixic acid, antibiotics that have been used in aquaculture practices but are not authorized for
194 use in Greece (Xu et al., 2022). Furthermore, the strains were resistant to 2% sodium lactate,
195 tetrazolium blue, and some antibiotics such as fusidic acid and rifamycin SV. Except for 23 carbon
196 sources utilization and 9 chemical resistance reactions that were constant for all the strains tested,
197 the other 62 reactions were variable. This aspect of the genus has been observed for many species,
198 and phenotypic identification must be complemented with genomic information (Thompson et al.,
199 2004). The Gen III MicroPlate assay results for carbon sources utilization and chemical resistance
200 are presented in **Table S1**.

201

202 3.2 Genomic characteristics, Pangenome and Phylogeny

203

204 The *V. harveyi* genome sizes and gene numbers among the strains were similar, with average
205 length of 6,009,731 bps dispersed across 63 to 232 contigs. GC content ranges from 43.63% to
206 44.93% (**Table 1**). On average, the number of genes annotated per strain was 5,570 (ranging from
207 5,259 to 6,082), with 5,495 of these being coding DNA sequences (CDSs) and 75 being RNA
208 sequences (ranging from 45 to 107). Among the annotated CDSs, an average of 664 hypothetical
209 proteins (ranging from 514 to 1,050) were identified across the 21 strains. Additionally, an average
210 of 66 pseudogenes (ranging from 28 to 106) were detected. The assembly did not provide
211 chromosome level results, but the statistics reveal good quality contigs with completeness 99.4%
212 and above, after BUSCO assessment, coverage around 203.69x and N50 between 228.328 and
213 507.658 (**Table S2**). The *V. harveyi* has been reported so far to possess two unequal in size
214 chromosomes as well as plasmids. The family Vibrionaceae is one of the families known to possess
215 chromids. This characteristic is associated with the plasticity of its bipartite genomes. The second
216 chromosome, typically approximately 2 Mb, is considered a chromid. In *Vibrio* species, both the
217 chromosome and chromid are similarly prone to gene acquisition (Sonnenberg and Haugen, 2023).
218 Chromids appear more often to eukaryote symbionts or pathogens (diCenzo and Finan, 2017). In
219 multipartite genomes, chromids have been attributed to facilitating bacteria in specific ecological
220 niches (diCenzo and Finan, 2017; Riccardi et al., 2023). A limitation of our study is that both short-
221 read sequencing and *de novo* assembly methods do not necessarily provide complete plasmid
222 sequences. Furthermore, the PLACNETw tool failed to identify any nodes recognized as plasmids.
223 Despite this, plasmids have been identified in complete genomes of the species, with sizes ranging
224 from 9 to 185 kbps (Montánchez and Kaberdin, 2020). Examination of the public NCBI database

225 (accessed on 2024/02/09), which included 29 complete genomes of *V. harveyi* and their associated
226 plasmids, revealed that the genome lengths exhibited a similar range to our findings, regardless of
227 the presence of plasmids.

228 The pangenome consists of 10,418 CDSs, 4,336 core, 3,030 dispensable, 3,053 singletons (**Figure**
229 **S1**). The pangenome of the 21 strains comprised approximately 6.5% hypothetical proteins, while
230 a similar proportion, around 7.5% of the core genome's CDSs, were found to have unknown
231 functions. The average number of singletons per isolate was 94, and the largest strain-specific gene
232 sets were found in the strains SA 6.1 and SS 1, with 199 and 376 genes, respectively. Most the
233 CDSs are either core or singletons and very few dispensable are shared between more than 4 strains
234 (**Table S3**). As additional genomes were incorporated into the dataset, the pangenome exhibited
235 continuous expansion without reaching a plateau (**Figure 1a**). Conversely, the core genome
236 decreased as the number of genomes increased along the x-axis. (**Figure 1b**). A similar
237 phenomenon has been observed in *Vibrio alginolyticus*, where strains from various geographic
238 regions and fish species also display an open pangenome (Chibani et al., 2020). The pangenome
239 evolution *V. harveyi* is characterized by gene gain/loss (De Mesa et al., 2023; Kayansamruaj et
240 al., 2018) and therefore the pangenome model is open, this is the case also for the 21 strains.
241 Species occupying diverse niches with many community interactions tend to have open
242 pangenomes where ecological factors are the key to bacterial gene sharing (Brockhurst et al.,
243 2019). Also, bipartite genomes of vibrios tend to be more open than monopartite genomes of
244 related families, therefore they are more prone to gene acquisition (Sonnenberg and Haugen,
245 2023).

246 All strains, including the ATCC 33843 reference strain, exhibited close relatedness, with pairwise
247 Average Nucleotide Identity (ANI) values exceeding 99%. The construction of the phylogenetic

248 tree for the 21 genomes was based on a core gene set comprising 4,336 genes (**Figure 2**). The
249 analysis formed three distinct major clusters. The Percentage of Conserved Proteins (POCP)
250 matrix closely matched the approximately maximum-likelihood tree in terms of the extent of small
251 groups with higher percentage identities (**Figure S2**). Specifically, Kef 80 exhibited a closer
252 relationship with MDO 7.2, Kef 22 with VhP1-li and ML 1, and Gal 88 with SM1. Importantly,
253 this clustering did not reflect geographic, temporal, or host source factors. In general, the high
254 protein similarities and conserved regions observed are characteristic of the species (Espinoza-
255 Valles et al., 2015). This explains why strains separated by both years and geographic distances
256 tend to cluster together.

257 The allele assignments within the PubMLST database for *gyrB*, *pyrH*, *recA*, and *atpA* displayed
258 significant diversity among the 21 strains, as detailed in **Table S4**, resulting in the classification
259 of distinct Sequence Types (STs). Among these strains, FL 9.1 was associated with ST=241, while
260 Serfr was linked to ST=216. Notably, both STs were attributed to *V. harveyi* isolates originating
261 from live marine animals located north of the Yangtze River, as well as other regions in Qingdao
262 and Hebei Provinces, China, spanning the years 2009 to 2016.

263

264 3.3 Metabolic enzymes, Virulence Factors, and HGT, from genotype to phenotype

265

266 Most of core genome proteins were found to be associated with COG superfamilies, with the most
267 prominent groups falling into three major categories: transcription, amino acid and carbohydrate
268 transport and metabolism (**Figure 3**). In contrast, fewer genes from the dispensable and singleton
269 fraction could be confidently assigned to the COG database. Interestingly, functions unique to

270 specific strains appeared to be primarily associated with processes such as replication, cell wall
271 and membrane formation, envelope biogenesis, intracellular trafficking, and the presence of
272 transposase elements.

273 The core genome of the strains encompassed crucial virulence factors, including transporters,
274 secretion systems, bacterial toxins, motility proteins, exosome proteins, antimicrobial resistance
275 mechanisms, prokaryotic defense systems, and siderophores. It is noteworthy that important
276 virulence elements are conserved within the core genome of *Vibrionaceae*, indicating that many
277 *Vibrio* species and strains in marine environments possess a fundamental repertoire of genetic tools
278 for potentially expressing pathogenic traits (Lilburn et al., 2010). However, it is important to
279 highlight that while numerous essential virulence factors were part of the core genome, singleton
280 gene sets also contained a subset of such factors (**Table S5**). This phenomenon is not uncommon
281 among pathogenic strains (Deng et al., 2019). For instance, SA 6.1 and SS 1, that exhibited the
282 largest singleton gene sets, contained genes that regulated processes such as metabolism,
283 transporters, two-component systems, quorum sensing and secretion systems.

284 Particularly important gene clusters of the T2SS, T3SS, T4SS, T6SS, T1SS, protein-export
285 proteins of the Sec-SRP system and flagellar-assembly proteins have been annotated. T3SS and
286 T6SS are closely associated with the pathogenicity of the species (Deng et al., 2019). Genes of
287 these systems are clustered together and share the same synteny in most of the genomes studied in
288 Fu *et al.*, who also incorporated the previous version of VH2 genome (Fu et al., 2021). This pattern
289 was observed in all 21 genomes as well. In addition to genes scattered throughout the genome, the
290 T3SS exhibited synteny with approximately 44 CDSs spanning 36.5 kbps in all 21 strains, while
291 the T6SS occupied 24.5 kbps.

292 The toxin genes in the core genome include an enterotoxin, the microbial collagenase *colA*
293 (K01387), the exfoliative toxin A/B *eta* (K11041), several lipases and phospholipases. Hemolytic
294 activity is very important for vibrios during infection (Ruwandeeepika et al., 2012). Some
295 hemolysins of the core genome are the thermolabile hemolysin *tlh* (K11018) and the hemolysin III
296 *hlyIII* (K11068) the *tlyC* (K03699), hemolysin family protein. There are two loci of thermolabile
297 hemolysin in two strains, VhP1sp and SD1.1, with the second being a fragment, while most of the
298 strains contained one copy. However, more copies do not indicate higher hemolytic activity (Zhang
299 et al., 2001). No hemolysins were detected in the singletons. All strains were capable of β -
300 hemolysis (**Figure S3**). RTX toxin genes were found in the singletons of VhP1-li. It is a finding
301 that could be associated with higher mortalities induced by this strain to the gilthead seabream
302 larvae in the *in vivo* test (**Figure 4**). The *rtx* genes are detected in conserved areas of *V. harveyi*
303 (Espinoza-Valles et al., 2015) and between tandem repeats that complicate the assembly of short-
304 read sequencing (Tørresen et al., 2019). Therefore, the lack of these loci in the other genomes,
305 such as ML 1, might be attributed to sequencing/assembly error.

306 Iron uptake operon and vibrioferrin-related proteins, located in chromosome II, are conserved in
307 the species (Espinoza-Valles et al., 2015). In the 21 genomes, the MotA/TolQ/ExbB siderophore
308 complex is conserved and detected inside a cluster of related proteins. *V. harveyi* regulates the
309 accumulation of siderophores during growth phases through quorum sensing (QS) (McRose et al.,
310 2018). Other iron binding and transport proteins involved the FeO system, ferric ion ABC
311 transporters, and the enterobactin biosynthesis protein, *fecB*. All strains contain genes for the
312 metabolism of terpenoids, polyketides, xenobiotics, and hydrogen-peroxide-resistance proteins
313 such as *oxyR*. Urease activity in *Vibrio parahaemolyticus* serves as a mechanism for modulating
314 the pH within their habitat (Berutti et al., 2014). This capability is particularly significant during

315 the colonization of a host, whether as symbionts or pathogens, as it enables the bacterium to
316 influence the pH levels within its environment to establish a favorable ecological niche. *V. harveyi*
317 also demonstrates ureolytic activity (Defoirdt et al., 2017). Specifically, all 21 strains were found
318 to contain the genes *ureG/F/C/B*, and in some strains, additional *ureF/D/A* genes were identified.
319 Furthermore, the presence of the *chbG* chitinase gene, along with other genes related to chitin
320 metabolism, was observed. This observation is significant, as it suggests that *V. harveyi* possesses
321 a genetic toolkit for utilizing chitin, which allows it to adapt to a diverse range of environmental
322 conditions (Ran et al., 2023).

323 In all the strains examined, various virulence factors included genes associated with the
324 thioredoxin (TRX) system, which plays a role in maintaining redox homeostasis, as well as global
325 regulators like *luxR*, *luxS*, and *luxP*, known for their involvement in QS and luminescence. Quorum
326 sensing, a regulatory mechanism, plays a crucial role in controlling virulence in bacteria of the
327 Harveyi clade (Zhang et al., 2023) and anti-phage defense systems (Tesson and Bernheim, 2023).
328 Although vibrios are generally recognized as luminous marine bacteria with a conserved *lux*
329 operon (Vannier et al., 2020), which was primarily associated with *Vibrio campbellii*, it is
330 noteworthy that in this collection of strains, only VarA4 1.1 exhibited luminescence on MA.
331 Surprisingly, neither the entire *lux* operon (*luxCDABFEG*) nor individual genes from the operon
332 were detected in any of the genomes. The presence or absence of the *lux* operon is linked to
333 symbiotic and planktonic lifestyles in bacteria, with non-luminescent isolates typically lacking this
334 operon (O'Grady and Wimpee, 2008). The *V. harveyi* strains are serious pathogens, but
335 bioluminescence is not correlated with virulence (Defoirdt et al., 2008). The *luxT*, that encodes a
336 small RNA that regulates QS response (Eickhoff et al., 2021), was present in the strains Kef 62,
337 Kef 75, ML 1, Serfr, SD 1.1, SA 9.1 and VH2 and the luciferase only in the Gal 1. Aldehyde

338 metabolism genes were detected in all strains. Aldehyde serves as substrate for luciferase, playing
339 a biochemical role in light emission observed in many *Vibrio* species (Dunlap, 2014).

340 Antimicrobial resistance genes (ARGs) are prevalent in bacteria of the aquatic environment and
341 can be identified in many aquaculture pathogens (Bondad-Reantaso et al., 2023). A comprehensive
342 global study on ocean resistomes revealed that approximately 25% of ARGs are found within
343 putative plasmid sequences, with the majority residing on bacterial chromosomes (Cuadrat et al.,
344 2020). This underscores the critical role of both resistant bacteria dissemination and horizontal
345 gene transfer in the spread of antimicrobial resistance. In the case of the 21 strains under
346 investigation, the presence of ARGs was relatively limited, but as the strains are characterized by
347 an open pangenome and the ability to receive incoming ARGs from other species is still a major
348 concern. Deng et al. similarly observed a constrained distribution of ARGs among collected *V.*
349 *harveyi* isolates (Deng et al., 2020). Some ARGs were detected in the core genome of the 21
350 strains, including blaCARB (blaCARB-17, K19217), the outer-membrane protein tolC (K12340),
351 and genes homologous to parS (K18072), which are associated with beta-lactam and cationic
352 antimicrobial peptide (CAMP) resistance. The blaCARB-17 locus is believed to be an intrinsic
353 chromosomal gene of *V. parahaemolyticus*, conferring resistance to β -lactams (Chiou et al., 2015).
354 While isolates carrying *tet* and *qnr* genes are common in aquaculture, they do not exhibit high
355 levels of resistance to tetracyclines and quinolones (Deng et al., 2020). Interestingly, all the
356 examined strains were found to harbor *catB* (K00638), *tet35* (K18218), and *qnr* (K18555) genes.
357 ARGs display temporal patterns among the replicons, chromosomes and plasmids. Notably,
358 certain genes, such as β -lactamases and *tet* efflux pumps, tend to be prevalent on specific types of
359 chromids. Efflux pumps are typically part of the core genome (Wang et al., 2022), and demonstrate
360 multifunctional characteristics. The multidrug efflux pump modules annotated in the strains shared

361 homology to *mexA* (K03585), *mexB* (K18138), *mexL* (K18301), *mexJ* (K18302), *cueR* (K19591),
362 and *oprN* (K18300). When assessing the disk diffusion diameters, it was observed that the strains
363 displayed resistance to ampicillin and, for the most part, sensitivity to the tested antibiotics (**Table**
364 **2**). Due to the absence of established zone diameter breakpoints for the antibiotics tested against
365 *V. harveyi*, classification of strains based on inhibition zones was not feasible in our study.
366 Recently, epidemiological cut-off values for these antibiotics and the species have been published,
367 that range from ≤ 0.5 to $9.5 \mu\text{g ml}^{-1}$ (Smith et al., 2023). Additionally, the supplementation of NaCl
368 in agar media has been subject to controversy (Smith, 2019; Smith and Egan, 2018), and
369 standardized protocols recommend unmodified MHA for this species. These limitations
370 underscore the challenges encountered in antimicrobial susceptibility testing and emphasize the
371 need for further research in this area. Only Kef 75 exhibited resistance to oxytetracycline and
372 sulfamethoxazole/trimethoprim, without the presence of any other known antibiotic resistance
373 genes (ARGs) to account for this resistance. *Vibrio* strains can exhibit diverse antibiotic resistance
374 profiles, complicating disease management strategies (Deekshit et al., 2023; Rigos and Kogiannou,
375 2023). While ampicillin is commonly not effective, most antibiotics tested displayed low
376 resistance, a trend observed in Croatian isolates from European seabass (Pavlinec et al., 2022) and
377 Italian *Vibrio* isolates from shellfish (Mancini et al., 2023). It is worth noting that AMR of *V.*
378 *harveyi* appears to pose a more severe challenge in shrimp aquaculture in regions such as China
379 and Malaysia, where higher multiple antibiotic resistance (MAR) indices have been reported
380 (Deekshit et al., 2023; Yu et al., 2023).

381 The present study did not assume a direct and unequivocal correlation between genotype and
382 phenotype, a presumption that often proves challenging to uphold, even when employing
383 computational models and genome-wide analyses (GWAs) (Lees et al., 2020). For example, the

384 presence of genes associated with specific metabolic phenotypes, such as the positive ornithine
385 decarboxylase reaction, D-galactose, and sucrose fermentation (**Table S6**), was not predicted in
386 the 21 *V. harveyi* strains as observed in strains 1792 and 14126T (Amaral et al., 2014). Predicting
387 genotype-to-phenotype relationships is generally more reliable in cases involving antibiotic
388 resistance, while for virulence, it is imperative to also consider the influence of epistasis (Sailer
389 and Harms, 2017). Furthermore, many virulence factors were detected in the core genome of the
390 21 strains. However, their pathogenicity against seabream larvae was different (**Figure S4, Table**
391 **S7, S8**) and the strains were clustered according to their pathogenic potential (**Figure 4**). In the
392 virulence assay conducted, strain ML 1 emerged as the most virulent, resulting in approximately
393 80% larval mortality over the five-day period. In contrast, strain Kef 75 exhibited the lowest
394 virulence, causing less than 10% mortality. The strains can be broadly categorized into three
395 groups based on their virulence levels: the most virulent group (classified as “g” to “efg”),
396 comprising the top three strains; the intermediate group (classified as “def” to “abcd”), consisting
397 of twelve strains with moderate virulence; and the least virulent group (classified as “abc” to “a”),
398 comprising seven strains with the lowest virulence. This classification highlights the varying
399 degrees of pathogenicity among the tested strains. Harboring the same virulence genes did not
400 translate to equal morbidity. The 21 strains had most of the main virulence genes mentioned in Fu
401 *et al.*, except for *mshB* and *hutR* (Fu et al., 2021), but it is uncertain if the lack of them would affect
402 virulence. The three most virulent strains derive from eastern Aegean, ML1 and VhP1-li are
403 phylogenetically closer and showed high percentage of conserved proteins. It is important to
404 acknowledge that the diverse origins of the strains, particularly in relation to the host species, may
405 influence the observed variations in morbidity outcomes. Different hosts would exhibit distinct
406 mortality gradients when exposed to the same strain (Firmino et al., 2019). For example, certain

407 fish species like the European seabass are known to be more susceptible to *V. harveyi* infections
408 (Pujalte et al., 2003), which may account for the higher number of isolates obtained from this
409 species in this study. Our findings also suggest that strains of *V. harveyi* exhibit differential
410 behavior depending on the host, underscoring the complexity of host-pathogen interactions.
411 Further investigations are needed to elucidate the underlying mechanisms governing host
412 specificity and pathogenicity in this bacterium.

413 The genomic islands accounted for approximately 10% of the total genome in these strains, as
414 indicated in Table 3. The mean length of these GIs was estimated at approximately 16.4 kbps, and
415 the coding sequences (CDSs) within them encompassed a diverse array of genetic elements. These
416 elements included ABC transporters, transcription regulators, proteins associated with antibiotic
417 resistance and hydrogen peroxide resistance, toxin-antitoxin systems, metabolic enzymes, and
418 approximately 37% of hypothetical proteins. Notably, the presence of a natural competence-
419 inducing factor Tfox/Sxy family protein was annotated in the genomes, linking the ability to grow
420 on chitin with HGT (Meibom et al., 2005). Vibrios exhibit remarkable genetic adaptability,
421 characterized by genetic exchanges within and between species in the marine environment (Le
422 Roux and Blokesch, 2018; Lilburn et al., 2010). HGT plays a pivotal role in this adaptability,
423 allowing the exchange of genetic material and contributing to genetic diversity. It involves the
424 transfer of genes related to virulence and antibiotic resistance, often through prophage regions and
425 plasmids (Ruwandeeepika et al., 2010). This genetic plasticity has enabled vibrios, such as *V.*
426 *harveyi*, to infect a broad spectrum of hosts, although rapid mutation rates have also influenced
427 their evolution (Thompson et al., 2004).

428 Moreover, each strain was found to possess a few prophage regions, with an average length of
429 approximately 19.7 kbps, as detailed in **Table 3**. Among these regions, the only intact prophage

430 was one of the strain Gal 1, comprising 63 CDSs (**Table S9**). Upon further analysis through a
431 BLAST search, it was revealed that this region exhibited significant similarity to chromosome two
432 of other *V. harveyi* strains isolated from fish (specific data not shown), and it shared common
433 synteny with an induced prophage from a *V. alginolyticus* strain obtained from a crab farm,
434 designated as Vibrio phage vB_ValM-yong1 (**Figure 5**) (Qin et al., 2021). The annotations within
435 the intact prophage of Gal 1 included a hemolysin domain, *phrB*, a TonB-dependent receptor, and
436 several phage-related proteins. In *V. harveyi*, lysogenic conversion has been known to enhance
437 virulence, either by introducing new toxins or by regulating host virulence factors (Nawel et al.,
438 2022). The study of microbe-host interactions has expanded to encompass microbe-microbe-host
439 /microbe-phage-host interactions. These inter-species interactions reveal exchanges not only of
440 virulence factors through horizontal gene transfer but also of anti-phage systems (Blokesch, 2021;
441 McDonald et al., 2019). In *Vibrio*, 88% of defense systems lie in genomic islands (McDonald et
442 al., 2019). In the 21 genomes, 47% of the defense systems predicted lied inside GIs (**Table S10**).
443 Multiple defense systems can target the same phage or confer resistance against different phages,
444 the clustering of these antiviral systems into defense islands may not only facilitate horizontal
445 transfer but also enable simultaneous regulation, providing a synergistic effect (Tesson and
446 Bernheim, 2023).

447 Some genomes of this study exhibited elements of potential CRISPR/Cas type I, and Cas type I-E
448 systems identified (**Table S11**). Specifically, one CRISPR element of approximately 75 base pairs
449 was detected in FL 9.1 and Gal 90, while *cas3*, *cse2*, and *casB* genes were dispersed within the
450 contigs of eight additional strains. The CRISPR/Cas type I-E system, originally described in *Vibrio*
451 *cholerae*, has been identified in 10 *Vibrio* and 4 *Photobacterium* species (McDonald et al., 2019).
452 In *V. harveyi*, the system is often found within a GI alongside T3SS genes, often occupying a

453 single locus, although it may be absent in certain strains (McDonald et al., 2019; Parra et al., 2021).
454 It is important to note that having a complete set of *cas* genes is not the standard for the genus, as
455 CRISPR/Cas systems are not evenly distributed among vibrios. Orphan genes may represent
456 fragments of functional systems or serve alternative functions (Baliga et al., 2019).

457

458 **4. Conclusions**

459

460 The 21 *V. harveyi* strains demonstrate predominantly consistent sensitivity to aquaculture
461 antibiotics, alongside varied metabolic profiles across multiple traits and diverse outcomes in
462 virulence assays. Moreover, their pangenome exhibits an open structure characterized by
463 numerous mobile elements and a broad array of virulence genes. It is imperative to maintain
464 continuous whole-genome sequencing efforts to monitor and evaluate the evolutionary
465 trajectory of these bacteria concerning disease. The genetic and phenotypic pathogenic
466 properties observed in these strains underscore the likelihood of *V. harveyi* remaining a
467 significant concern for Greek aquaculture in the foreseeable future.

468

469 **5. Funding**

470

471 This work was supported by the Greek General Secretariat of Research and Technology under the
472 Operational Program Competitiveness, Entrepreneurship and Innovation 2014-2020, grant number
473 MIS5045915; Z.A.I was supported by the Erasmus+ Key Action 1- Erasmus Mundus Joint Master

474 (EMJM) [Project No.: 101080968, Topic: ERASMUS-EDU-2022-PEX-EMJM-MOB for the
475 EMJMD in Aquaculture, Environment and Society STAR (EMJMD ACES-STAR)].

476

477 **6. Acknowledgements**

478

479 This work is dedicated to the late Dr. Panos Varvarigos, whose active contributions to the project,
480 encompassing both intellectual insights and practical inputs, were invaluable to our research
481 endeavors. His legacy continues to inspire us.

482

483 **7. References**

484

485 Adams, D., Boopathy, R., 2013. Use of formic acid to control vibriosis in shrimp aquaculture. *Biologia*
486 (Bratisl) 68, 1017–1021. <https://doi.org/10.2478/s11756-013-0251-x>

487 Amaral, G.R.S., Dias, G.M., Wellington-Oguri, M., Chimetto, L., Campeão, M.E., Thompson, F.L.,
488 Thompson, C.C., 2014. Genotype to phenotype: identification of diagnostic vibrio phenotypes using
489 whole genome sequences. *Int J Syst Evol Microbiol* 64, 357–365.
490 <https://doi.org/10.1099/ijs.0.057927-0>

491 Arias-Andres, M., Klümper, U., Rojas-Jimenez, K., Grossart, H.-P., 2018. Microplastic pollution increases
492 gene exchange in aquatic ecosystems. *Environmental Pollution* 237, 253–261.
493 <https://doi.org/10.1016/j.envpol.2018.02.058>

494 Arndt, D., Grant, J.R., Marcu, A., Sajed, T., Pon, A., Liang, Y., Wishart, D.S., 2016. PHASTER: a better,
495 faster version of the PHAST phage search tool. *Nucleic Acids Res* 44, W16–W21.
496 <https://doi.org/10.1093/nar/gkw387>

497 Austin, B., Zhang, X.H., 2006. *Vibrio harveyi*: A significant pathogen of marine vertebrates and
498 invertebrates. *Lett Appl Microbiol* 43, 119–124. <https://doi.org/10.1111/j.1472-765X.2006.01989.x>

499 Baker-Austin, C., Trinanes, J., Gonzalez-Escalona, N., Martinez-Urtaza, J., 2017. Non-Cholera Vibrios:
500 The Microbial Barometer of Climate Change. *Trends Microbiol.*
501 <https://doi.org/10.1016/j.tim.2016.09.008>

502 Baliga, P., Shekar, M., Venugopal, M.N., 2019. Investigation of direct repeats, spacers and proteins
503 associated with clustered regularly interspaced short palindromic repeat (CRISPR) system of *Vibrio*
504 *parahaemolyticus*. *Molecular Genetics and Genomics* 294, 253–262. [https://doi.org/10.1007/s00438-](https://doi.org/10.1007/s00438-018-1504-8)
505 [018-1504-8](https://doi.org/10.1007/s00438-018-1504-8)

506 Bertelli, C., Laird, M.R., Williams, K.P., Lau, B.Y., Hoad, G., Winsor, G.L., Brinkman, F.S., 2017.
507 IslandViewer 4: expanded prediction of genomic islands for larger-scale datasets. *Nucleic Acids Res*
508 45, W30–W35. <https://doi.org/10.1093/nar/gkx343>

509 Berutti, T.R., Williams, R.E., Shen, S., Taylor, M.M., Grimes, D.J., 2014. Prevalence of urease in *Vibrio*
510 *parahaemolyticus* from the Mississippi Sound. *Lett Appl Microbiol* 58, 624–628.
511 <https://doi.org/10.1111/lam.12237>

512 Blokesch, M., 2021. Growing away from monocultures – interdependent growth conditions for studying
513 antibacterial and antiphage systems. *Environ Microbiol Rep* 13, 42–44. [https://doi.org/10.1111/1758-](https://doi.org/10.1111/1758-2229.12899)
514 [2229.12899](https://doi.org/10.1111/1758-2229.12899)

515 Bondad-Reantaso, M.G., MacKinnon, B., Karunasagar, Iddya, Fridman, S., Alday-Sanz, V., Brun, E., Le
516 Groumellec, M., Li, A., Surachetpong, W., Karunasagar, Indrani, Hao, B., Dall’Occo, A., Urbani, R.,

517 Caputo, A., 2023. Review of alternatives to antibiotic use in aquaculture. *Rev Aquac.*
518 <https://doi.org/10.1111/raq.12786>

519 Bowley, J., Baker-Austin, C., Porter, A., Hartnell, R., Lewis, C., 2021. Oceanic Hitchhikers – Assessing
520 Pathogen Risks from Marine Microplastic. *Trends Microbiol* 29, 107–116.
521 <https://doi.org/10.1016/j.tim.2020.06.011>

522 Brenner, D.J., Krieg, N.R., Staley, J.T., Garrity, G.M., Boone, D.R., de Vos, P., Goodfellow, M., Rainey,
523 F.A., Schleifer, K.-H. (Eds.), 2005. *Bergey's Manual® of Systematic Bacteriology*, 2nd ed. Springer
524 US, Boston, MA. <https://doi.org/10.1007/0-387-28022-7>

525 Brockhurst, M.A., Harrison, E., Hall, J.P.J., Richards, T., McNally, A., MacLean, C., 2019. The Ecology
526 and Evolution of Pangenomes. *Current Biology*. <https://doi.org/10.1016/j.cub.2019.08.012>

527 Castillo, D., D'Alvise, P., Middelboe, M., Gram, L., Liu, S., Kalatzis, P.G., Kokkari, C., Katharios, P.,
528 2015. Draft genome sequences of the fish pathogen *Vibrio harveyi* strains VH2 and VH5. *Genome*
529 *Announc* 3, 2–4. <https://doi.org/10.1128/genomeA.01062-15>

530 Chen, L., 2004. VFDB: a reference database for bacterial virulence factors. *Nucleic Acids Res* 33, D325–
531 D328. <https://doi.org/10.1093/nar/gki008>

532 Chibani, C.M., Roth, O., Liesegang, H., Wendling, C.C., 2020. Genomic variation among closely related
533 *Vibrio alginolyticus* strains is located on mobile genetic elements. *BMC Genomics* 21, 1DUMM.
534 <https://doi.org/10.1186/s12864-020-6735-5>

535 Chiou, J., Li, R., Chen, S., 2015. CARB-17 family of β -lactamases mediates intrinsic resistance to
536 penicillins in *Vibrio parahaemolyticus*. *Antimicrob Agents Chemother* 59, 3593–3595.
537 <https://doi.org/10.1128/AAC.00047-15>

538 Chuchird, N., Rorkwiree, P., Rairat, T., 2015. Effect of dietary formic acid and astaxanthin on the survival
539 and growth of Pacific white shrimp (*Litopenaeus vannamei*) and their resistance to *Vibrio*
540 *parahaemolyticus*. Springerplus 4, 440. <https://doi.org/10.1186/s40064-015-1234-x>

541 CLSI, 2016. Methods for Antimicrobial Dilution and Disk Susceptibility Testing of Infrequently Isolated
542 or Fastidious Bacteria. 3rd ed. CLSI Guideline M45. Wayne, PA: Clinical and Laboratory Standards
543 Institute.

544 Couvin, D., Bernheim, A., Toffano-Nioche, C., Touchon, M., Michalik, J., Néron, B., Rocha, E.P.C.,
545 Vergnaud, G., Gautheret, D., Pourcel, C., 2018. CRISPRCasFinder, an update of CRISRFinder,
546 includes a portable version, enhanced performance and integrates search for Cas proteins. *Nucleic*
547 *Acids Res* 46, W246–W251. <https://doi.org/10.1093/nar/gky425>

548 Cuadrat, R.R.C., Sorokina, M., Andrade, B.G., Goris, T., Dávila, A.M.R., 2020. Global ocean resistome
549 revealed: Exploring antibiotic resistance gene abundance and distribution in TARA Oceans samples.
550 *Gigascience* 9. <https://doi.org/10.1093/gigascience/giaa046>

551 Cui, Y., Chen, X., Luo, H., Fan, Z., Luo, J., He, S., Yue, H., Zhang, P., Chen, R., 2016. BioCircos.js: an
552 interactive Circos JavaScript library for biological data visualization on web applications.
553 *Bioinformatics* 32, 1740–2. <https://doi.org/10.1093/bioinformatics/btw041>

554 Danecek, P., Bonfield, J.K., Liddle, J., Marshall, J., Ohan, V., Pollard, M.O., Whitwham, A., Keane, T.,
555 McCarthy, S.A., Davies, R.M., Li, H., 2021. Twelve years of SAMtools and BCFtools. *Gigascience*
556 10. <https://doi.org/10.1093/gigascience/giab008>

557 Davis, J.J., Wattam, A.R., Aziz, R.K., Brettin, T., Butler, R., Butler, R.M., Chlenski, P., Conrad, N.,
558 Dickerman, A., Dietrich, E.M., Gabbard, J.L., Gerdes, S., Guard, A., Kenyon, R.W., Machi, D., Mao,
559 C., Murphy-Olson, D., Nguyen, M., Nordberg, E.K., Olsen, G.J., Olson, R.D., Overbeek, J.C.,
560 Overbeek, R., Parrello, B., Pusch, G.D., Shukla, M., Thomas, C., VanOeffelen, M., Vonstein, V.,
561 Warren, A.S., Xia, F., Xie, D., Yoo, H., Stevens, R., 2019. The PATRIC Bioinformatics Resource

562 Center: expanding data and analysis capabilities. *Nucleic Acids Res.*
563 <https://doi.org/10.1093/nar/gkz943>

564 De Mesa, C.A., Mendoza, R.M., Penir, S.M.U., de la Peña, L.D., Amar, E.C., Saloma, C.P., 2023. Genomic
565 analysis of *Vibrio harveyi* strain PH1009, a potential multi-drug resistant pathogen due to acquisition
566 of toxin genes. *Heliyon* 9. <https://doi.org/10.1016/j.heliyon.2023.e14926>

567 Deekshit, V.K., Maiti, B., Krishna Kumar, B., Kotian, A., Pinto, G., Bondad-Reantaso, M.G., Karunasagar,
568 Iddya, Karunasagar, Indrani, 2023. Antimicrobial resistance in fish pathogens and alternative risk
569 mitigation strategies. *Rev Aquac.* <https://doi.org/10.1111/raq.12715>

570 Defoirdt, T., Verstraete, W., Bossier, P., 2008. Luminescence, virulence and quorum sensing signal
571 production by pathogenic *Vibrio campbellii* and *Vibrio harveyi* isolates. *J Appl Microbiol* 104, 1480–
572 1487. <https://doi.org/10.1111/j.1365-2672.2007.03672.x>

573 Defoirdt, T., Vlaeminck, S.E., Sun, X., Boon, N., Clauwaert, P., 2017. Ureolytic Activity and Its Regulation
574 in *Vibrio campbellii* and *Vibrio harveyi* in Relation to Nitrogen Recovery from Human Urine. *Environ*
575 *Sci Technol* 51, 13335–13343. <https://doi.org/10.1021/acs.est.7b03829>

576 Deng, Y., Xu, H., Su, Y., Liu, S., Xu, L., Guo, Z., Wu, J., Cheng, C., Feng, J., 2019. Horizontal gene
577 transfer contributes to virulence and antibiotic resistance of *Vibrio harveyi* 345 based on complete
578 genome sequence analysis. *BMC Genomics* 20. <https://doi.org/10.1186/s12864-019-6137-8>

579 Deng, Y., Xu, L., Liu, S., Wang, Q., Guo, Z., Chen, C., Feng, J., 2020a. What drives changes in the virulence
580 and antibiotic resistance of *Vibrio harveyi* in the South China Sea? *J Fish Dis* jfd.13197.
581 <https://doi.org/10.1111/jfd.13197>

582 Deng, Y., Xu, L., Liu, S., Wang, Q., Guo, Z., Chen, C., Feng, J., 2020b. What drives changes in the
583 virulence and antibiotic resistance of *Vibrio harveyi* in the South China Sea? *J Fish Dis* jfd.13197.
584 <https://doi.org/10.1111/jfd.13197>

585 diCenzo, G.C., Finan, T.M., 2017. The Divided Bacterial Genome: Structure, Function, and Evolution.
586 Microbiology and Molecular Biology Reviews 81. <https://doi.org/10.1128/membr.00019-17>

587 Dieckmann, M.A., Beyvers, S., Nkouamedjo-Fankep, R.C., Hanel, P.H.G., Jelonek, L., Blom, J.,
588 Goesmann, A., 2021. EDGAR3.0: comparative genomics and phylogenomics on a scalable
589 infrastructure. Nucleic Acids Res 49, W185–W192. <https://doi.org/10.1093/nar/gkab341>

590 Droubogiannis, S., Katharios, P., 2022. Genomic and Biological Profile of a Novel Bacteriophage, Vibrio
591 phage Virtus, Which Improves Survival of Sparus aurata Larvae Challenged with Vibrio harveyi.
592 Pathogens 11. <https://doi.org/10.3390/pathogens11060630>

593 Dunlap, P., 2014. Biochemistry and Genetics of Bacterial Bioluminescence. pp. 37–64.
594 https://doi.org/10.1007/978-3-662-43385-0_2

595 Edgar, R.C., 2004. MUSCLE: multiple sequence alignment with high accuracy and high throughput.
596 Nucleic Acids Res 32, 1792–1797. <https://doi.org/10.1093/nar/gkh340>

597 Eickhoff, M.J., Fei, C., Huang, X., Bassler, B.L., 2021. LuxT controls specific quorum-sensing-regulated
598 behaviors in Vibrionaceae spp. via repression of qrr1, encoding a small regulatory RNA. PLoS Genet
599 17, e1009336. <https://doi.org/10.1371/journal.pgen.1009336>

600 Espinoza-Valles, I., Vora, G.J., Lin, B., Leekitcharoenphon, P., González-Castillo, A., Ussery, D., Høj, L.,
601 Gomez-Gil, B., 2015a. Unique and conserved genome regions in Vibrio harveyi and related species
602 in comparison with the shrimp pathogen Vibrio harveyi CAIM 1792. Microbiology (United Kingdom)
603 161, 1762–1779. <https://doi.org/10.1099/mic.0.000141>

604 Espinoza-Valles, I., Vora, G.J., Lin, B., Leekitcharoenphon, P., González-Castillo, A., Ussery, D., Høj, L.,
605 Gomez-Gil, B., 2015b. Unique and conserved genome regions in Vibrio harveyi and related species
606 in comparison with the shrimp pathogen Vibrio harveyi CAIM 1792. Microbiology (United Kingdom)
607 161, 1762–1779. <https://doi.org/10.1099/mic.0.000141>

608 Firmino, J., Furones, M.D., Andree, K.B., Sarasquete, C., Ortiz-Delgado, J.B., Asencio-Alcudia, G.,
609 Gisbert, E., 2019. Contrasting outcomes of *Vibrio harveyi* pathogenicity in gilthead seabream, *Sparus*
610 *aurata* and European seabass, *Dicentrarchus labrax*. *Aquaculture* 511, 734210.
611 <https://doi.org/10.1016/j.aquaculture.2019.734210>

612 Fu, S., Ni, P., Yang, Q., Hu, H., Wang, Q., Ye, S., Liu, Y., 2021. Delineating the key virulence factors and
613 intraspecies divergence of *Vibrio harveyi* via whole-genome sequencing. *Can J Microbiol* 67, 231–
614 248. <https://doi.org/10.1139/cjm-2020-0079>

615 Jolley, K.A., Bray, J.E., Maiden, M.C.J., 2018. Open-access bacterial population genomics: BIGSdb
616 software, the PubMLST.org website and their applications. *Wellcome Open Res* 3, 124.
617 <https://doi.org/10.12688/wellcomeopenres.14826.1>

618 Kanehisa, M., Sato, Y., Morishima, K., 2016. BlastKOALA and GhostKOALA: KEGG Tools for
619 Functional Characterization of Genome and Metagenome Sequences. *J Mol Biol* 428, 726–731.
620 <https://doi.org/10.1016/j.jmb.2015.11.006>

621 Kayansamruaj, P., Dong, H.T., Hirono, I., Kondo, H., Senapin, S., Rodkhum, C., 2018. Genome
622 characterization of piscine ‘Scale drop and Muscle Necrosis syndrome’-associated strain of *Vibrio*
623 *harveyi* focusing on bacterial virulence determinants. *J Appl Microbiol* 124, 652–666.
624 <https://doi.org/10.1111/jam.13676>

625 Le Roux, F., Blokesch, M., 2018a. Eco-evolutionary Dynamics Linked to Horizontal Gene Transfer in
626 *Vibrios*. *Annu Rev Microbiol* 72, 89–110. <https://doi.org/10.1146/annurev-micro-090817-062148>

627 Le Roux, F., Blokesch, M., 2018b. Eco-evolutionary Dynamics Linked to Horizontal Gene Transfer in
628 *Vibrios*. *Review in Advance*. <https://doi.org/10.1146/annurev-micro-090817>

629 Le Roux, F., Wegner, K.M., Baker-Austin, C., Vezzulli, L., Osorio, C.R., Amaro, C., Ritchie, J.M.,
630 Defoirdt, T., Destoumieux-Garzón, D., Blokesch, M., Mazel, D., Jacq, A., Cava, F., Gram, L.,

631 Wendling, C.C., Strauch, E., Kirschner, A., Huehn, S., 2015. The emergence of *Vibrio* pathogens in
632 Europe: ecology, evolution, and pathogenesis. *Front Microbiol* 6, 11–12.
633 <https://doi.org/10.3389/fmicb.2015.00830>

634 Lee, J.-H., Lee, J., 2010. Indole as an intercellular signal in microbial communities. *FEMS Microbiol Rev*
635 34, 426–444. <https://doi.org/10.1111/j.1574-6976.2009.00204.x>

636 Lees, J.A., Mai, T.T., Galardini, M., Wheeler, N.E., Horsfield, S.T., Parkhill, J., Corander, J., 2020.
637 Improved Prediction of Bacterial Genotype-Phenotype Associations Using Interpretable Pangenome-
638 Spanning Regressions. *mBio* 11, e01344-20. <https://doi.org/10.1128/mBio.01344-20>

639 Li, W., O’Neill, K.R., Haft, D.H., DiCuccio, M., Chetvernin, V., Badretdin, A., Coulouris, G., Chitsaz, F.,
640 Derbyshire, M.K., Durkin, A.S., Gonzales, N.R., Gwadz, M., Lanczycki, C.J., Song, J.S., Thanki, N.,
641 Wang, J., Yamashita, R.A., Yang, M., Zheng, C., Marchler-Bauer, A., Thibaud-Nissen, F., 2021.
642 RefSeq: expanding the Prokaryotic Genome Annotation Pipeline reach with protein family model
643 curation. *Nucleic Acids Res* 49, D1020–D1028. <https://doi.org/10.1093/nar/gkaa1105>

644 Li, X., Yang, Q., Dierckens, K., Milton, D.L., Defoirdt, T., 2014. RpoS and Indole Signaling Control the
645 Virulence of *Vibrio anguillarum* towards Gnotobiotic Sea Bass (*Dicentrarchus labrax*) Larvae. *PLoS*
646 *One* 9, e111801. <https://doi.org/10.1371/journal.pone.0111801>

647 Lilburn, T.G., Gu, J., Cai, H., Wang, Y., 2010. Comparative genomics of the family Vibrionaceae reveals
648 the wide distribution of genes encoding virulence-associated proteins. *BMC Genomics* 11.
649 <https://doi.org/10.1186/1471-2164-11-369>

650 Mancini, M.E., Alessiani, A., Donatiello, A., Didonna, A., D’Attoli, L., Faleo, S., Occhiochiuso, G.,
651 Carella, F., Di Taranto, P., Pace, L., Rondinone, V., Damato, A.M., Coppola, R., Pedarra, C.,
652 Goffredo, E., 2023. Systematic Survey of *Vibrio* spp. and *Salmonella* spp. in Bivalve Shellfish in
653 Apulia Region (Italy): Prevalence and Antimicrobial Resistance. *Microorganisms* 11.
654 <https://doi.org/10.3390/microorganisms11020450>

655 McDonald, N.D., Regmi, A., Morreale, D.P., Borowski, J.D., Fidelma Boyd, E., 2019. CRISPR-Cas
656 systems are present predominantly on mobile genetic elements in *Vibrio* species. *BMC Genomics* 20.
657 <https://doi.org/10.1186/s12864-019-5439-1>

658 McRose, D.L., Baars, O., Seyedsayamdost, M.R., Morel, F.M.M., 2018. Quorum sensing and iron regulate
659 a two-for-one siderophore gene cluster in *Vibrio harveyi*. *Proc Natl Acad Sci U S A* 115, 7581–7586.
660 <https://doi.org/10.1073/pnas.1805791115>

661 Meibom, K.L., Blokesch, M., Dolganov, N.A., Wu, C.-Y., Schoolnik, G.K., 2005. Chitin Induces Natural
662 Competence in *Vibrio cholerae*. *Science* (1979) 310, 1824–1827.
663 <https://doi.org/10.1126/science.1120096>

664 Mohamad, N., Amal, M.N.A., Yasin, I.S.M., Zamri Saad, M., Nasruddin, N.S., Al-saari, N., Mino, S.,
665 Sawabe, T., 2019. Vibriosis in cultured marine fishes: a review. *Aquaculture* 512, 734289.
666 <https://doi.org/10.1016/j.aquaculture.2019.734289>

667 Mohd Yazid, S.H., Mohd Daud, H., Azmai, M.N.A., Mohamad, N., Mohd Nor, N., 2021. Estimating the
668 Economic Loss Due to Vibriosis in Net-Cage Cultured Asian Seabass (*Lates calcarifer*): Evidence
669 From the East Coast of Peninsular Malaysia. *Front Vet Sci* 8.
670 <https://doi.org/10.3389/fvets.2021.644009>

671 Montánchez, I., Kaberdin, V.R., 2020. *Vibrio harveyi*: A brief survey of general characteristics and recent
672 epidemiological traits associated with climate change. *Mar Environ Res* 154.
673 <https://doi.org/10.1016/j.marenvres.2019.104850>

674 Mougín, J., Roquigny, R., Flahaut, C., Bonnín-Jusserand, M., Grard, T., Le Bris, C., 2021. Abundance and
675 spatial patterns over time of Vibrionaceae and *Vibrio harveyi* in water and biofilm from a seabass
676 aquaculture facility. *Aquaculture* 542, 736862. <https://doi.org/10.1016/j.aquaculture.2021.736862>

677 Mueller, R.S., Beyhan, S., Saini, S.G., Yildiz, F.H., Bartlett, D.H., 2009. Indole Acts as an Extracellular
678 Cue Regulating Gene Expression in *Vibrio cholerae*. *J Bacteriol* 191, 3504–3516.
679 <https://doi.org/10.1128/JB.01240-08>

680 Nawel, Z., Rima, O., Amira, B., 2022. An overview on *Vibrio* temperate phages: Integration mechanisms,
681 pathogenicity, and lysogeny regulation. *Microb Pathog* 165, 105490.
682 <https://doi.org/10.1016/j.micpath.2022.105490>

683 Nogales, B., Lanfranconi, M.P., Piña-Villalonga, J.M., Bosch, R., 2011. Anthropogenic perturbations in
684 marine microbial communities. *FEMS Microbiol Rev* 35, 275–298. [https://doi.org/10.1111/j.1574-](https://doi.org/10.1111/j.1574-6976.2010.00248.x)
685 [6976.2010.00248.x](https://doi.org/10.1111/j.1574-6976.2010.00248.x)

686 O’Grady, E.A., Wimpee, C.F., 2008. Mutations in the *lux* Operon of Natural Dark Mutants in the Genus
687 *Vibrio*. *Appl Environ Microbiol* 74, 61–66. <https://doi.org/10.1128/AEM.01199-07>

688 Parra, A.E., Antequera, L., Lossada, C.A., Fernández-Materán, F. V., Parra, M.M., Centanaro, P., Arcos,
689 D., Castro, A., Moncayo, L.S., Romero, F., Paz, J.L., Vera-Villalobos, J., Pérez, A.E., Alvarado, Y.J.,
690 González-Paz, L.A., 2021. Comparative analysis of crispr-cas systems in *vibrio* and *photobacterium*
691 genomes of high influence in aquaculture production. *Biointerface Res Appl Chem* 11, 9513–9529.
692 <https://doi.org/10.33263/BRIAC112.95139529>

693 Pavlinec, Ž., Zupičić, I.G., Oraić, D., Lojkić, I., Fouz, B., Zrnčić, S., 2022. Biochemical and molecular
694 characterization of three serologically different *Vibrio harveyi* strains isolated from farmed
695 *Dicentrarchus labrax* from the Adriatic Sea. *Sci Rep* 12, 7309. [https://doi.org/10.1038/s41598-022-](https://doi.org/10.1038/s41598-022-10720-z)
696 [10720-z](https://doi.org/10.1038/s41598-022-10720-z)

697 Pujalte, M.J., Sitjà-Bobadilla, A., Macián, M.C., Belloch, C., Álvarez-Pellitero, P., Pérez-Sánchez, J.,
698 Uruburu, F., Garay, E., 2003. Virulence and Molecular Typing of *Vibrio harveyi* Strains Isolated from
699 Cultured Dentex, Gilthead Sea Bream and European Sea Bass. *Syst Appl Microbiol* 26, 284–292.
700 <https://doi.org/10.1078/072320203322346146>

701 Qin, Q.-L., Xie, B.-B., Zhang, X.-Y., Chen, X.-L., Zhou, B.-C., Zhou, J., Oren, A., Zhang, Y.-Z., 2014. A
702 Proposed Genus Boundary for the Prokaryotes Based on Genomic Insights. *J Bacteriol* 196, 2210–
703 2215. <https://doi.org/10.1128/JB.01688-14>

704 Qin, W., Li, D., Xu, L., Lin, W., Tong, Y., 2021. Complete genome analysis of an active prophage of *Vibrio*
705 *alginolyticus*. *Arch Virol* 166, 891–896. <https://doi.org/10.1007/s00705-020-04941-8>

706 Ran, L., Wang, X., He, X., Guo, R., Wu, Y., Zhang, P., Zhang, X.-H., 2023. Genomic analysis and chitinase
707 characterization of *Vibrio harveyi* WXL538: insight into its adaptation to the marine environment.
708 *Front Microbiol* 14. <https://doi.org/10.3389/fmicb.2023.1121720>

709 Riccardi, C., Koper, P., Innocenti, G., Dicenzo, G.C., Fondi, M., Mengoni, A., Perrin, E., 2023. Independent
710 origins and evolution of the secondary replicons of the class Gammaproteobacteria. *Microb Genom*
711 9. <https://doi.org/10.1099/mgen.0.001025>

712 Riegert, A.S., Narindoshvili, T., Coricello, A., Richards, N.G.J., Raushel, F.M., 2021. Functional
713 Characterization of Two PLP-Dependent Enzymes Involved in Capsular Polysaccharide Biosynthesis
714 from *Campylobacter jejuni*. *Biochemistry* 60, 2836–2843.
715 <https://doi.org/10.1021/acs.biochem.1c00439>

716 Rigos, G., Kogiannou, D., 2023. Antimicrobial drugs in aquaculture: use and abuse, in: Knowles, M.E.,
717 Anelich, L.E., Boobis, A.R., Popping, B. (Eds.), *Present Knowledge in Food Safety*. Academic Press,
718 pp. 142–161. <https://doi.org/10.1016/B978-0-12-819470-6.00027-5>

719 Roberts, R.J. (Ed.), 2012. *Fish Pathology*, 4th ed. Wiley-Blackwell, Oxford.
720 <https://doi.org/10.1002/9781118222942>

721 Rodriguez-R, L., Konstantinidis, K., 2016. The enveomics collection: a toolbox for specialized analyses of
722 microbial genomes and metagenomes. *PeerJ Prepr* 4, e1900v1.
723 <https://doi.org/10.7287/peerj.preprints.1900v1>

724 Ruwandeepika, H.A.D., Defoirdt, T., Bhowmick, P.P., Shekar, M., Bossier, P., Karunasagar, I., 2010.
725 Presence of typical and atypical virulence genes in vibrio isolates belonging to the Harveyi clade. *J*
726 *Appl Microbiol* 109, 888–899. <https://doi.org/10.1111/j.1365-2672.2010.04715.x>

727 Ruwandeepika, H.A.D., Jayaweera, P.S., Bhowmick, P.P., Karunasagar, I., Bossier, P., Defoirdt, T., 2012.
728 Pathogenesis, virulence factors and virulence regulation of vibrios belonging to the Harveyi clade.
729 *Rev Aquac* 4, 59–74. <https://doi.org/10.1111/j.1753-5131.2012.01061.x>

730 Sailer, Z.R., Harms, M.J., 2017. Detecting high-order epistasis in nonlinear genotype-phenotype maps.
731 *Genetics* 205, 1079–1088. <https://doi.org/10.1534/genetics.116.195214>

732 Sampaio, A., Silva, V., Poeta, P., Aonofriesei, F., 2022. *Vibrio* spp.: Life Strategies, Ecology, and Risks in
733 a Changing Environment. *Diversity (Basel)* 14, 97. <https://doi.org/10.3390/d14020097>

734 Saulnier, D., de Decker, S., Haffner, P., Cobret, L., Robert, M., Garcia, C., 2010. A large-scale
735 epidemiological study to identify bacteria pathogenic to Pacific Oyster *Crassostrea gigas* and
736 correlation between virulence and metalloprotease-like activity. *Microb Ecol* 59, 787–798.
737 <https://doi.org/10.1007/s00248-009-9620-y>

738 Sawabe, T., Inoue, S., Fukui, Y., Yoshie, K., Nishihara, Y., Miura, H., 2007. Mass Mortality of Japanese
739 Abalone *Haliotis discus hannai* Caused by *Vibrio harveyi* Infection. *Microbes Environ* 22, 300–308.
740 <https://doi.org/10.1264/jsme2.22.300>

741 Simão, F.A., Waterhouse, R.M., Ioannidis, P., Kriventseva, E. V., Zdobnov, E.M., 2015. BUSCO: assessing
742 genome assembly and annotation completeness with single-copy orthologs. *Bioinformatics* 31, 3210–
743 3212. <https://doi.org/10.1093/bioinformatics/btv351>

744 Smith, P., 2019. THE PERFORMANCE OF ANTIMICROBIAL SUSCEPTIBILITY TESTING
745 PROGRAMMES RELEVANT TO AQUACULTURE AND AQUACULTURE PRODUCTS, in:
746 *FAO Fisheries and Aquaculture Circular N.C1191* . Rome.

747 Smith, P., Cortinovis, L., Pretto, T., Manfrin, A., Florio, D., Fioravanti, M., Baron, S., Le Devendec, L.,
748 Jouy, E., Le Breton, A., Picon-Camacho, S., Zupičić, I.G., Oraić, D., Zrnčić, S., 2023. Setting
749 epidemiological cut-off values for *Vibrio harveyi* relevant to MIC data generated by a standardised
750 microdilution method. *Dis Aquat Organ* 155, 35–42. <https://doi.org/10.3354/dao03740>

751 Smith, P., Egan, S., 2018. Standard protocols for antimicrobial susceptibility testing of Vibrionaceae
752 isolated from aquatic animals, *Bull. Eur. Ass. Fish Pathol.*

753 Sonnenberg, C.B., Haugen, P., 2023. Bipartite Genomes in Enterobacterales: Independent Origins of
754 Chromids, Elevated Openness and Donors of Horizontally Transferred Genes. *Int J Mol Sci* 24.
755 <https://doi.org/10.3390/ijms24054292>

756 Tesson, F., Bernheim, A., 2023. Synergy and regulation of antiphage systems: toward the existence of a
757 bacterial immune system? *Curr Opin Microbiol* 71, 102238.
758 <https://doi.org/10.1016/j.mib.2022.102238>

759 Tesson, F., Hervé, A., Mordret, E., Touchon, M., D’Humières, C., Cury, J., Bernheim, A., 2022. Systematic
760 and quantitative view of the antiviral arsenal of prokaryotes. *Nat Commun* 13, 2561.
761 <https://doi.org/10.1038/s41467-022-30269-9>

762 Thompson, F.L., Iida, T., Swings, J., 2004. Biodiversity of Vibrios. *Microbiology and Molecular Biology*
763 *Reviews* 68, 403–431. <https://doi.org/10.1128/MMBR.68.3.403-431.2004>

764 Tørresen, O.K., Star, B., Mier, P., Andrade-Navarro, M.A., Bateman, A., Jarnot, P., Gruca, A., Grynberg,
765 M., Kajava, A. V, Promponas, V.J., Anisimova, M., Jakobsen, K.S., Linke, D., 2019. Tandem repeats
766 lead to sequence assembly errors and impose multi-level challenges for genome and protein databases.
767 *Nucleic Acids Res* 47, 10994–11006. <https://doi.org/10.1093/nar/gkz841>

768 Triga, A., Smyrli, M., Katharios, P., 2023. Pathogenic and Opportunistic *Vibrio* spp. Associated with
769 Vibriosis Incidences in the Greek Aquaculture: The Role of *Vibrio harveyi* as the Principal Cause of
770 Vibriosis. *Microorganisms* 11. <https://doi.org/10.3390/microorganisms11051197>

771 Tsertou, M.I., Triga, A., Droubogiannis, S., Kokkari, C., Anasi, G., Katharios, P., 2023. Isolation and
772 characterization of a novel *Tenacibaculum* species and a corresponding bacteriophage from a
773 Mediterranean fish hatchery: Description of *Tenacibaculum larymnensis* sp. nov. and *Tenacibaculum*
774 phage Larrie. *Front Microbiol* 14. <https://doi.org/10.3389/fmicb.2023.1078669>

775 Vannier, T., Hingamp, P., Turrel, F., Tanet, L., Lescot, M., Timsit, Y., 2020. Diversity and evolution of
776 bacterial bioluminescence genes in the global ocean. *NAR Genom Bioinform* 2.
777 <https://doi.org/10.1093/nargab/lqaa018>

778 Vielva, L., de Toro, M., Lanza, V.F., de la Cruz, F., 2017. PLACNETw: a web-based tool for plasmid
779 reconstruction from bacterial genomes. *Bioinformatics* 33, 3796–3798.
780 <https://doi.org/10.1093/bioinformatics/btx462>

781 Vinnitskiy, D.Z., Ustyuzhanina, N.E., Nifantiev, N.E., 2015. Natural bacterial and plant biomolecules
782 bearing α -d-glucuronic acid residues. *Russian Chemical Bulletin* 64, 1273–1301.
783 <https://doi.org/10.1007/s11172-015-1010-7>

784 Walker, B.J., Abeel, T., Shea, T., Priest, M., Abouelliel, A., Sakthikumar, S., Cuomo, C.A., Zeng, Q.,
785 Wortman, J., Young, S.K., Earl, A.M., 2014. Pilon: An Integrated Tool for Comprehensive Microbial
786 Variant Detection and Genome Assembly Improvement. *PLoS One* 9, e112963.
787 <https://doi.org/10.1371/journal.pone.0112963>

788 Wang, Y., Batra, A., Schulenburg, H., Dagan, T., 2022. Gene sharing among plasmids and chromosomes
789 reveals barriers for antibiotic resistance gene transfer. *Philosophical Transactions of the Royal Society*
790 *B: Biological Sciences* 377. <https://doi.org/10.1098/rstb.2020.0467>

791 Wick, R.R., Judd, L.M., Gorrie, C.L., Holt, K.E., 2017. Unicycler: Resolving bacterial genome assemblies
792 from short and long sequencing reads. PLoS Comput Biol 13.
793 <https://doi.org/10.1371/journal.pcbi.1005595>

794 Wick, R.R., Schultz, M.B., Zobel, J., Holt, K.E., 2015. Bandage: interactive visualization of de novo
795 genome assemblies: Fig. 1. Bioinformatics 31, 3350–3352.
796 <https://doi.org/10.1093/bioinformatics/btv383>

797 Xu, K., Wang, Y., Yang, W., Cai, H., Zhang, Y., Huang, L., 2022. Strategies for Prevention and Control of
798 Vibriosis in Asian Fish Culture. Vaccines (Basel) 11, 98. <https://doi.org/10.3390/vaccines11010098>

799 Yu, Y., Tang, M., Wang, Y., Liao, M., Wang, C., Rong, X., Li, B., Ge, J., Gao, Y., Dong, X., Zhang, Z.,
800 2023. Virulence and antimicrobial resistance characteristics assessment of *Vibrio* isolated from
801 shrimp (*Penaeus vannamei*) breeding system in south China. Ecotoxicol Environ Saf 252.
802 <https://doi.org/10.1016/j.ecoenv.2023.114615>

803 Zhang, S., Yang, Q., Defoirdt, T., 2022. Indole decreases the virulence of pathogenic vibrios belonging to
804 the *Harveyi* clade. J Appl Microbiol 132, 167–176. <https://doi.org/10.1111/jam.15227>

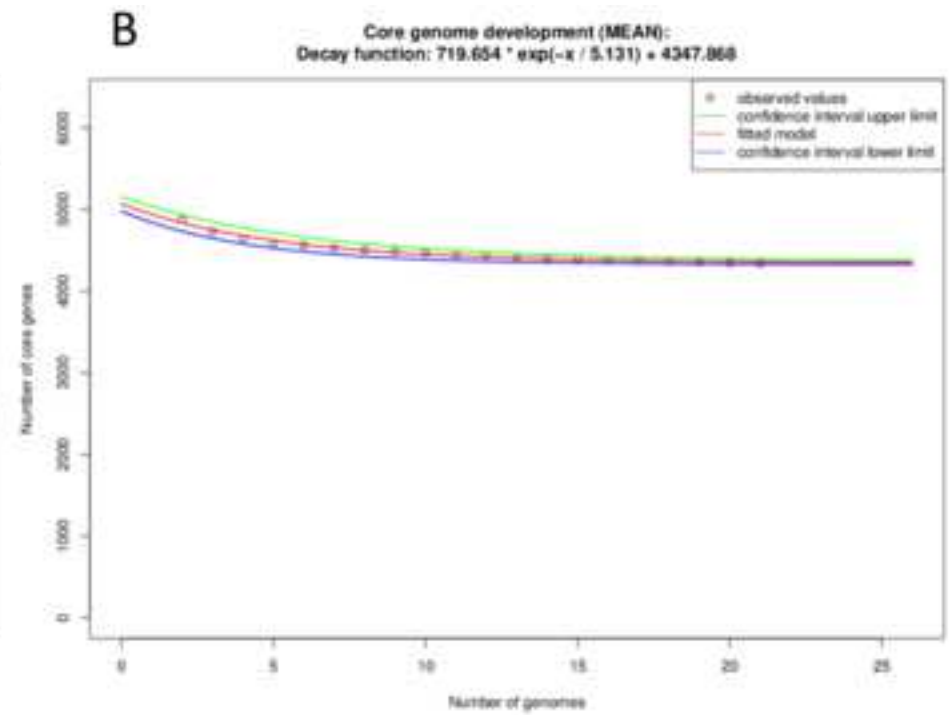
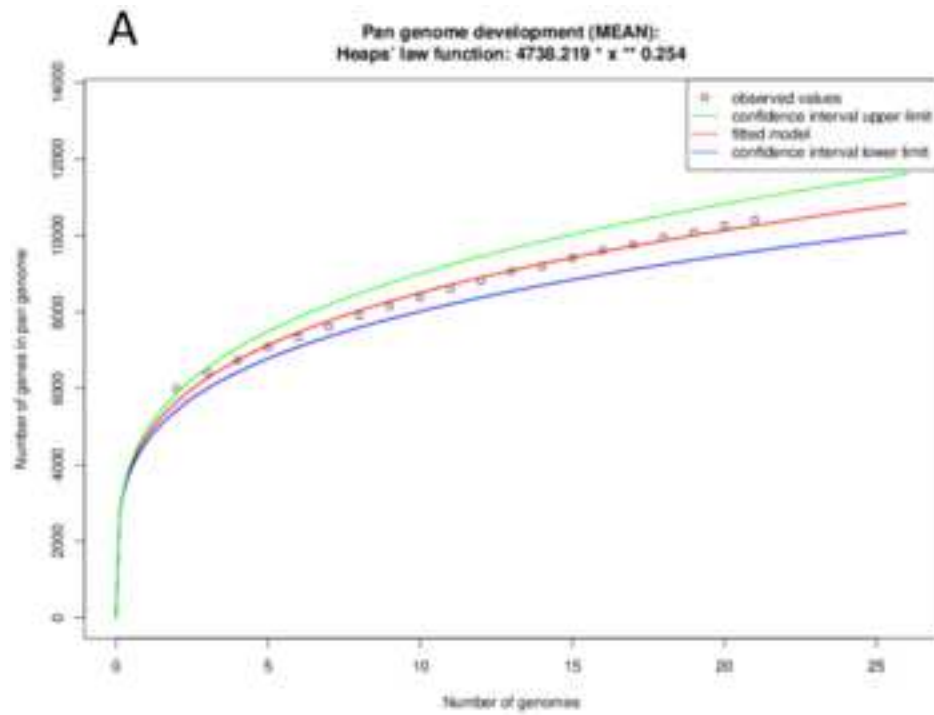
805 Zhang, S., Yang, Q., Eggermont, M., Defoirdt, T., 2023. Quorum- sensing interference in vibrios. Rev
806 Aquac. <https://doi.org/10.1111/raq.12787>

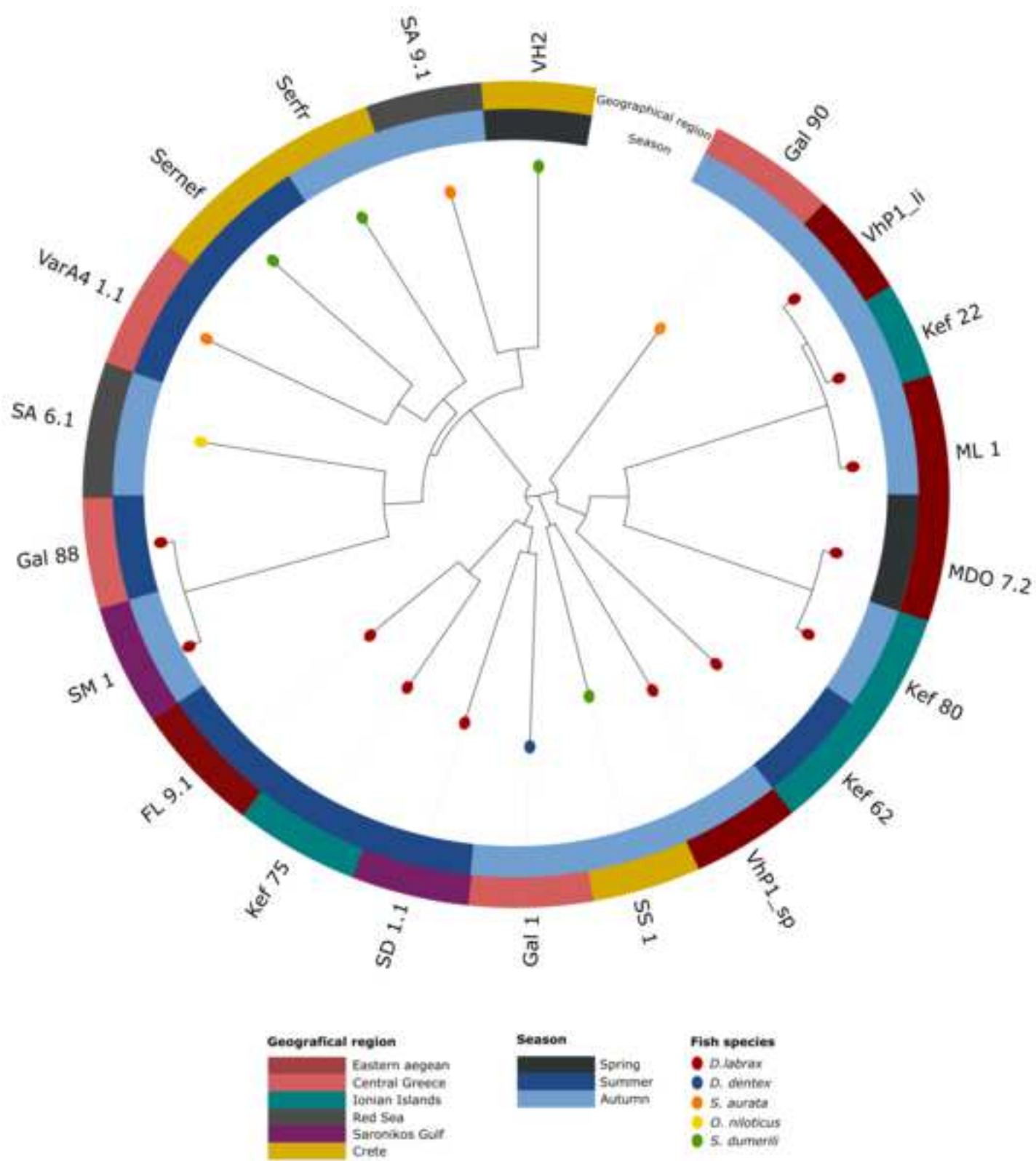
807 Zhang, X.-H., He, X., Austin, B., 2020. *Vibrio harveyi*: a serious pathogen of fish and invertebrates in
808 mariculture. Mar Life Sci Technol 2, 231–245. <https://doi.org/10.1007/s42995-020-00037-z>

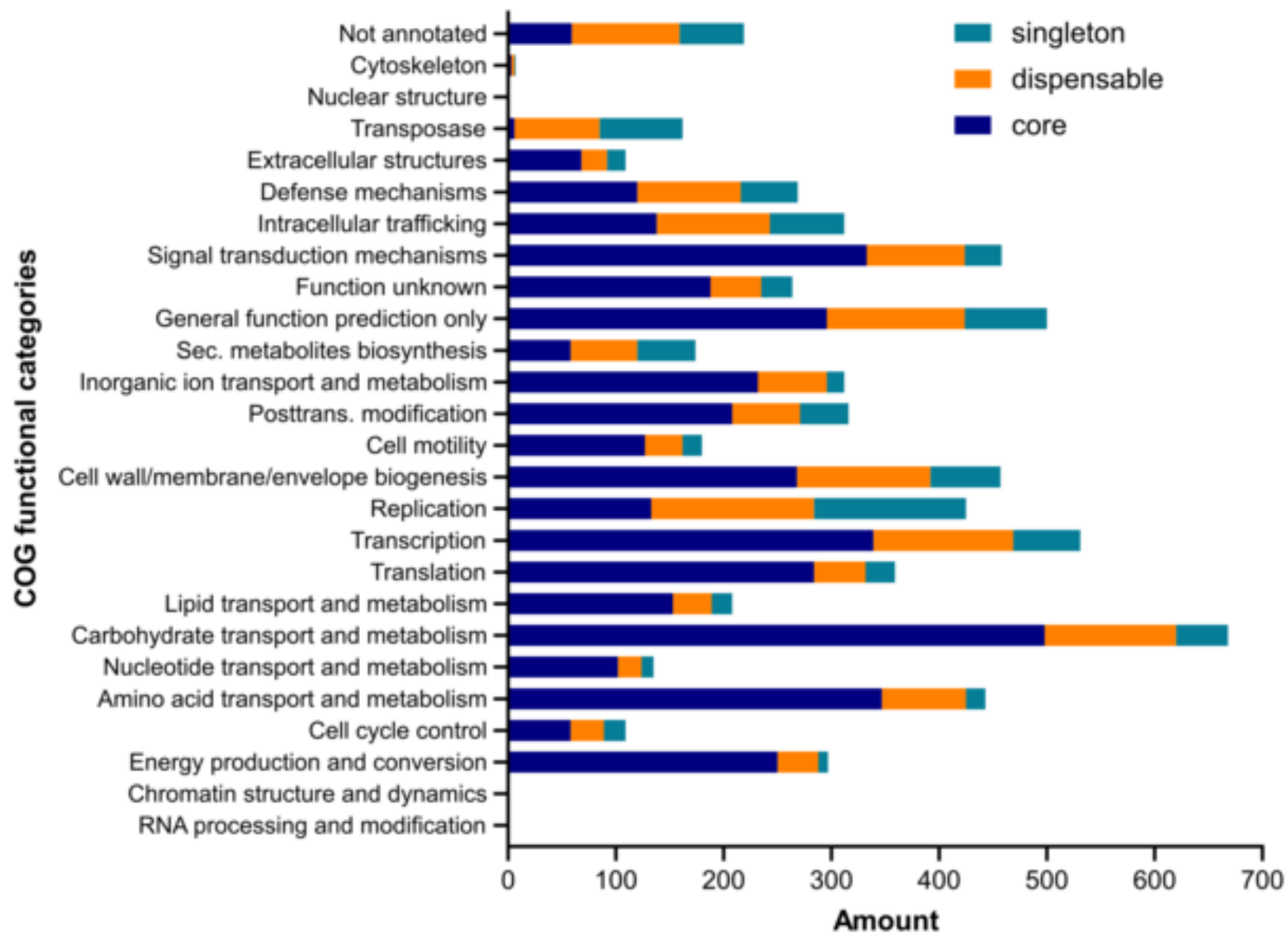
809 Zhang, X.-H., Meaden, P.G., Austin, B., 2001. Duplication of Hemolysin Genes in a Virulent Isolate of
810 *Vibrio harveyi*. Appl Environ Microbiol 67, 3161–3167. [https://doi.org/10.1128/AEM.67.7.3161-](https://doi.org/10.1128/AEM.67.7.3161-3167.2001)
811 [3167.2001](https://doi.org/10.1128/AEM.67.7.3161-3167.2001)

812

813







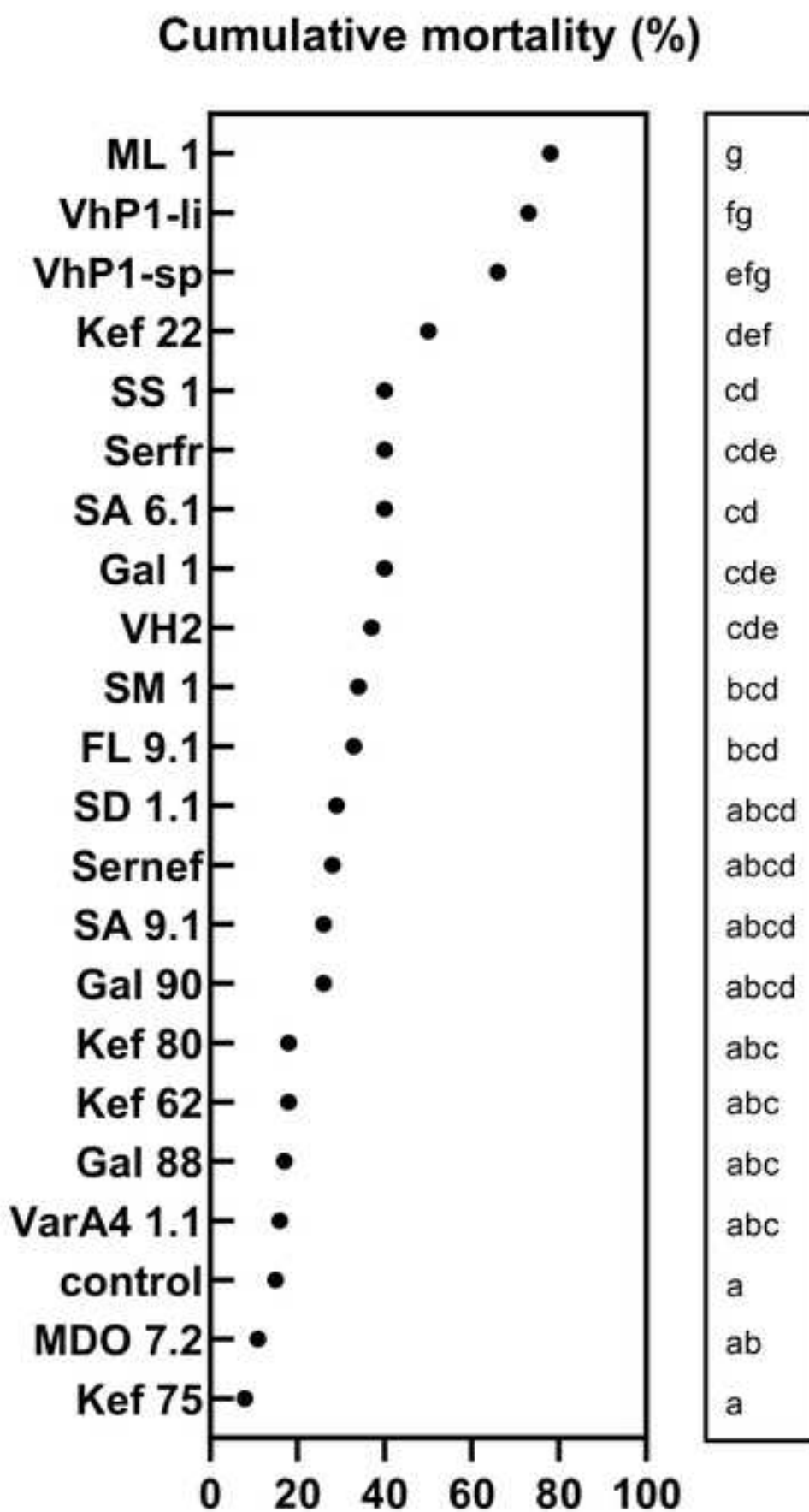


Figure 1. Curves showing the pangenome (A) and core genome (B) development for the 21 *V. harveyi* strains.

Figure 2. Phylogenetic tree of the 21 strains, constructed using the EDGAR platform based on core genes, with each genome consisting of 4,336 genes and a total of 1,411,553 amino acid residues. The outer ring represents the geographical origin of the strains, while the inner ring indicates the season of isolation. Host species are denoted by circles at the ends of the branches.

Figure 3. COG functional categories in the core, dispensable and singleton fractions of the pangenome.

Figure 4. Cumulative mortality percentages of seabream larvae at day 5 after virulence challenge with the 21 *V. harveyi* strains (n values available in Table S7). Following Log-rank (Mantel-Cox) analysis, letters indicate statistically significant difference of the pairwise comparisons ($p < 0.0001$) between all strains.

Figure 5. The LCB 2 (44 kbps) of the Mauve genome alignment of Gal 1 prophage region (sequence 1) and Vibrio phage vB_ValM-yong1 NC_049477 (sequence 2).

Table 1. Strain and genome information

| | Host (tissue) | Location (year) | Size (Mbp) | GC (%) |
|----------------|------------------------------|-----------------------------|-------------------|---------------|
| FL 9.1 | <i>D. labrax</i> (kidney) | North Aegean (2020) | 6.03 | 44.77 |
| Gal 1 | <i>D. dentex</i> (kidney) | Central Greece (2019) | 6.04 | 44.8 |
| Gal 88 | <i>D. labrax</i> (kidney) | Central Greece (2020) | 5.98 | 44.87 |
| Gal 90 | <i>S. aurata</i> (kidney) | Central Greece (2020) | 6.02 | 44.67 |
| Kef 22 | <i>D. labrax</i> (kidney) | Ionian Islands (2015) | 6.09 | 44.71 |
| Kef 62 | <i>D. labrax</i> (spleen) | Ionian Islands (2020) | 5.93 | 44.79 |
| Kef 75 | <i>D. labrax</i> (kidney) | Ionian Islands (2020) | 5.82 | 44.86 |
| Kef 80 | <i>D. labrax</i> (brain) | Ionian Islands (2020) | 6.02 | 44.82 |
| MDO 7.2 | <i>D. labrax</i> (kidney) | Eastern Aegean (2018) | 6.04 | 44.83 |
| ML 1 | <i>D. labrax</i> (kidney) | Eastern Aegean (2020) | 6.14 | 44.69 |
| SA 6.1 | <i>O. niloticus</i> (kidney) | Red Sea (2019) | 5.96 | 44.83 |
| SA 9.1 | <i>S. aurata</i> (kidney) | Red Sea (2019) | 5.93 | 44.89 |
| SD 1.1 | <i>D. labrax</i> (intestine) | Saronikos Gulf (2020) | 5.71 | 44.93 |
| Serfr | <i>S. dumerili</i> (fry) | Crete (2015) | 5.85 | 44.86 |
| Sernef | <i>S. dumerili</i> (kidney) | Crete (2017) | 5.99 | 44.77 |

| | | | | |
|------------------|-----------------------------|-----------------------------|------|-------|
| SM 1 | <i>S. dumerili</i> (kidney) | Saronikos Gulf (2019) | 6.39 | 44.6 |
| SS 1 | <i>S. dumerili</i> (kidney) | Crete (2021) | 6.39 | 43.63 |
| VarA4 1.1 | <i>S. aurata</i> (brain) | Central Greece (2019) | 5.86 | 44.78 |
| VH2 | <i>S. dumerili</i> (tail) | Crete (2015) | 5.74 | 44.93 |
| VhP1-li | <i>D. labrax</i> (liver) | Eastern Aegean (2015) | 6.14 | 44.71 |
| VhP1-sp | <i>D. labrax</i> (spleen) | Eastern Aegean (2015) | 6.14 | 44.74 |

| CDSs (total) | tRNA genes | rRNA genes | GenBank/RefSeq Accession (PGAP Accession) |
|---------------------|-------------------|-------------------|--|
| 5,523 | 67 | 3 | JAIQZG000000000 |
| 5,499 | 74 | 3 | JAIPUI000000000 |
| 5,439 | 66 | 4 | JAIQXQ000000000 |
| 5,505 | 68 | 3 | JAIULD000000000 |
| 5,587 | 69 | 3 | JAIULE000000000 |
| 5,360 | 38 | 3 | JAKGDN000000000 |
| 5,299 | 67 | 4 | JAKGDM000000000 |
| 5,455 | 64 | 3 | JAIULF000000000 |
| 5,461 | 64 | 3 | JAIVBD000000000 |
| 5,625 | 65 | 3 | JAIVBF000000000 |
| 5,461 | 61 | 3 | JAJIRZ000000000 |
| 5,405 | 78 | 4 | JAJISA000000000 |
| 5,191 | 69 | 3 | JAKGDL000000000 |
| 5,354 | 54 | 4 | JAKGDK000000000 |
| 5,571 | 78 | 3 | JAIVBG000000000 |

| | | | |
|-------|----|---|-----------------|
| 5,998 | 76 | 4 | JAIVBH000000000 |
| 5,898 | 98 | 4 | JAKGDJ000000000 |
| 5,328 | 70 | 4 | JAIWIV000000000 |
| 5,191 | 61 | 3 | JAIVBE000000000 |
| 5,642 | 63 | 3 | JAIWIX000000000 |
| 5,603 | 67 | 3 | JAIWIW000000000 |

Table 2. Antibiotic sensitivity of the 21 *V. harveyi* strains expressed in diameter of inhibition zones.

| (mm) | OT30 | OA2 | SXT25 | UB30 | FFC30 | AMP10 |
|-----------|------|-----|-------|------|-------|-------|
| FL 9.1 | 28 | 16 | 20 | 26 | 27 | 0 |
| Gal 1 | 23 | 18 | 22 | 26 | 28 | 0 |
| Gal 88 | 22 | 21 | 23 | 28 | 30 | 0 |
| Gal 90 | 20 | 15 | 21 | 25 | 29 | 0 |
| Kef 22 | 23 | 17 | 18 | 24 | 26 | 0 |
| Kef 62 | 25 | 18 | 25 | 28 | 28 | 0 |
| Kef 75 | 0 | 15 | 0 | 25 | 30 | 0 |
| Kef 80 | 23 | 16 | 20 | 22 | 28 | 0 |
| MDO7.2 | 23 | 14 | 17 | 21 | 24 | 0 |
| ML 1 | 24 | 17 | 21 | 25 | 28 | 0 |
| SA 6.1 | 24 | 19 | 23 | 28 | 32 | 0 |
| SA 9.1 | 24 | 16 | 21 | 24 | 30 | 0 |
| SD 1.1 | 27 | 18 | 22 | 30 | 28 | 0 |
| Serfr | 25 | 16 | 22 | 27 | 32 | 0 |
| Sernef | 24 | 16 | 20 | 25 | 29 | 0 |
| SM 1 | 29 | 25 | 29 | 34 | 35 | 0 |
| SS 1 | 21 | 21 | 21 | 30 | 29 | 0 |
| Var A41.1 | 23 | 16 | 22 | 25 | 35 | 0 |
| VH2 | 22 | 16 | 21 | 23 | 28 | 0 |
| VhP1-li | 25 | 19 | 22 | 27 | 30 | 0 |
| VhP1-sp | 25 | 17 | 20 | 25 | 30 | 0 |

Table 3. Genomic Islands and Prophage regions of the 21 *V.harveyi* strains.

| | GIs/ WG (%) | Average Length (kbps) | Sum of GIs (bps) |
|-------------------|--------------------|------------------------------|-------------------------|
| FL 9.1 | 11 | 18.8 | 658,640 |
| Gal 1 | 8 | 20.5 | 470,576 |
| Gal 88 | 6 | 18.8 | 376,174 |
| Gal 90 | 19 | 17.2 | 1,121,186 |
| Kef 22 | 13 | 13.2 | 804,665 |
| Kef 62 | 9 | 22 | 504,917 |
| Kef 75 | 4 | 15.6 | 218,399 |
| Kef 80 | 8 | 11.3 | 509,363 |
| MDO 7.2 | 9 | 10.7 | 533,721 |
| ML 1 | 13 | 12.9 | 812,241 |
| SA 6.1 | 12 | 14.5 | 739,727 |
| SA 9.1 | 9 | 12.2 | 510,603 |
| SD 1.1 | 9 | 11.9 | 560,875 |
| Serfr | 6 | 20.3 | 345,422 |
| Sernef | 6 | 19.9 | 378,737 |
| SM 1 | 13 | 16.2 | 827,530 |
| SS 1 | 11 | 23.6 | 708,587 |
| Var A4 1.1 | 11 | 19.1 | 668,102 |
| VH2 | 8 | 10.5 | 440,817 |
| VHP1-li | 11 | 20.3 | 690,589 |
| VHP1-sp | 9 | 16.1 | 548,906 |

WG: whole genome, hp: hypothetical proteins, a: strain Gal 1 has also 1 intact 55.7 kbps prophage, b:

| No. of hp in GIs/genes total (%) | No. of Incomplete Prophages | Average Length (kbps) |
|---|------------------------------------|------------------------------|
| 35 | 1 | 16.3 |
| 33 | 1 ^a | 12.9 |
| 37 | 3 | 8.2 |
| 40 | 1 | 30.8 |
| 36 | 2 | 18.4 |
| 35 | 1 | 30.9 |
| 33 | 2 | 31.2 |
| 30 | 1 | 30.8 |
| 33 | 1 | 12.9 |
| 34 | 1 | 27.5 |
| 38 | 4 | 18 |
| 40 | 1 | 14.4 |
| 45 | 3 | 9.5 |
| 37 | 4 | 8.2 |
| 38 | 2 | 19.1 |
| 53 | 2 | 26.2 |
| 49 | 2 ^b | 26.7 |
| 36 | 2 | 17.3 |
| 31 | 1 | 31.4 |
| 37 | 1 | 18.3 |
| 32 | 2 | 18.1 |

strain SS 1 has also 1 questionable 26.3 kbps prophage

Declaration of Interest Statement

The authors declare no conflict of interest, as this work was funded by European Union and government agencies.

The authors declare that this manuscript is original, has not been published previously, and is not currently being considered for publication elsewhere. Any sources of funding received for this research have been disclosed, and all conflicts of interest have been declared. The authors are accountable for the accuracy and integrity of the work presented herein.

CRediT author statement: Conceptualization: [A.T. and P.K.]; Methodology: [A.T., M.S., and P.K.]; Formal Analysis: [A.T., Z.A.I., M.S. and L.F.]; Investigation: [A.T., M.S., and P.K.]; Resources: [P.K.]; Data Curation: [A.T. and L.F.]; Writing - Original Draft Preparation: [A.T. and P.K.]; Writing - Review and Editing: [A.T., Z.A.I., L.F. and P.K.]; Supervision: [P.K.]; Project Administration: [P.K.]; Funding Acquisition: [Z.A.I and P.K.].